Accepted for publication in ISIJ International, 1999

Neural Networks in Materials Science

H. K. D. H. Bhadeshia

University of Cambridge

Department of Materials Science and Metallurgy

Pembroke Street, Cambridge CB2 3QZ, U.K.

hkdb@cus.cam.ac.uk www.msm.cam.ac.uk/phase–trans

ABSTRACT

There are difficult problems in materials science where the general concepts might be understood but which are not as yet amenable to scientific treatment. We are at the same time told that good engineering has the responsibility to reach objectives in a cost and time–effective way. Any model which deals with only a small part of the required technology is therefore unlikely to be treated with respect. Neural network analysis is a form of regression or classification modelling which can help resolve these difficulties whilst striving for longer term solutions. This paper begins with an introduction to neural networks and contains a review of some applications of the technique in the context of materials science.

Keywords: Neural networks, materials science, introduction, applications

INTRODUCTION

The development and processing of materials is complex. Although scientific investigations on materials have helped greatly in understanding the underlying phenomena, there remain many problems where quantitative treatments are dismally lacking. For example, whereas dislocation theory can be used to estimate the yield strength of a microstructure, it is not yet possible to predict the strain hardening coefficient of an engineering alloy. It follows that the tensile strength, elongation, fatigue life, creep life and toughness, all of which are vital engineering design parameters, cannot even be estimated using dislocation theory. A more comprehensive list of what needs to be done in this context is presented in Table 1.

The lack of progress in predicting mechanical properties is because of their dependence on large numbers of variables. Nevertheless, there are clear patterns which experienced metallurgists recognise and understand. For example, it is well understood that the toughness of a steel can be improved by making its microstructure more chaotic so that propagating cracks are frequently deflected. It is not clear exactly how much the toughness is expected to improve, but the qualitative relationship is well established on the basis of a vast number of experiments.

Neural network models are extremely useful in such circumstances, not only in the study of mechanical properties but wherever the complexity of the problem is overwhelming from a fundamental perspective and where simplification is unacceptable. The purpose of this review is to explain how vague ideas might be incorporated into quantitative models using the neural network methodology. We begin with an introduction to the method, followed by a review of its application to materials.

Property	Relevance
Yield strength	All structural applications
Ultimate tensile strength	All structural applications
YS/UTS ratio	Tolerance to plastic overload
Elongation	Resistance to brittle fracture
Uniform elongation	Related to YS and UTS
Non–uniform elongation	Related to inclusions
Toughness	Tolerance to defects
Fatigue	Cyclic loading, life assessments
Stress corrosion	Slow corrosion & cracking
Creep strength	High temperature service
Creep ductility	Safe design
Creep–fatigue	Fatigue at creep temperatures
Elastic modulus	Deflection, stored energy
Thermal expansivity	Thermal fatigue/stress/shock
Hardness	Tribological properties

Table 1: Mechanical properties that need to be expressed in quantitative models as a function of large numbers of variables.

PHYSICAL & EMPIRICAL MODELS

A good theory must satisfy at least two criteria. It must describe a large class of observations with few arbitrary parameters. And secondly, it must make predictions which can be verified or disproved. Physical models, such as the crystallographic theory of martensite [1,2], satisfy both of these requirements. Thus, it is possible to predict the habit plane, orientation relationship and shape deformation of martensite with a precision greater than that of most experimental techniques, from a knowledge of just the crystal structures of the parent and product phases. By contrast, a linear regression equation requires at least as many parameters as the number of variables to describe the experimental data, and the equation itself may not be physically justified. Neural networks fall in this second category of empirical models; we shall see that they have considerable advantages over linear regression. In spite of the large number of parameters usually necessary to define a trained network, they are useful in circumstances where physical models do not exist.

LINEAR REGRESSION

Most scientists are familiar with regression analysis where data are best–fitted to a specified relationship which is usually linear. The result is an equation in which each of the inputs x_j is multiplied by a weight w_j; the sum of all such products and a constant θ then gives an estimate of the output $y = \sum_j w_j x_j + \theta$. As an example, the temperature at which the bainite reaction starts (*i.e.* B_S) in steel may be written [3]:

$$B_S(^\circ\mathrm{C}) = \underbrace{830}_{\theta} \underbrace{-270}_{w_C} \times c_C \underbrace{-90}_{w_{Mn}} \times c_{Mn} \underbrace{-37}_{w_{Ni}} \times c_{Ni} \underbrace{-70}_{w_{Cr}} \times c_{Cr} \underbrace{-83}_{w_{Mo}} \times c_{Mo} \qquad (1)$$

where c_i is the wt% of element i which is in solid solution in austenite. The term w_i is then the best–fit value of the *weight* by which the concentration is multiplied; θ is a constant. Because the variables are assumed to be independent, this equation can be stated to apply for the concentration range:

Carbon	0.1-0.55 wt.%	Nickel	0.0-5.0
Silicon	0.1-0.35	Chromium	0.0-3.5
Manganese	0.2-1.7	Molybdenum	0.0-1.0

and for this range the bainite–start temperature can be estimated with 90% confidence to $\pm 25\,^{\circ}\mathrm{C}$.

Equation 1 assumes that there is a linear dependence of B_S on concentration †. It may also be argued that there is an interaction between carbon and molybdenum since the latter is a strong carbide forming element. This can be expressed by introducing an additional term as follows:

$$B_S\,^{\circ}\mathrm{C} = 830 - 270 \times c_C - 90 \times c_{Mn} - 37 \times c_{Ni} - 70 \times c_{Cr} - 83 \times c_{Mo} \underbrace{+22 \times (c_C \times c_{Mo})}_{\text{interaction}} \quad (2)$$

Of course, there is no justification for the choice of the particular form of relationship. This and other difficulties associated with ordinary linear regression analysis can be summarised as follows:

Difficulty (a) A relationship has to be chosen before analysis.

Difficulty (b) The relationship chosen tends to be linear, or with non–linear terms added together to form a psuedo-linear equation.

Difficulty (c) The regression equation, once derived, applies across the entire span of the input space. This may not be reasonable. For example, the relationship between strength and the carbon concentration of an iron–base alloy must change radically as steel gives way to cast iron.

NEURAL NETWORKS

A general method of regression which avoids these difficulties is neural network analysis, illustrated at first using the familiar linear regression method. A network representation of linear regression is illustrated in Fig. 1a. The inputs x_i (concentrations) define the *input nodes*, the bainite–start temperature the *output node*. Each input is multiplied by a random weight w_i and the products are summed together with a constant θ to give the output $y = \sum_i w_i x_i + \theta$. The summation is an operation which is hidden at the hidden node. Since the weights and the constant θ were chosen at random, the value of the output will not match with experimental data. The weights are systematically changed until a best–fit description of the output is obtained as a function of the inputs; this operation is known as *training* the network.

The network can be made non–linear as shown in Fig. 1b. As before, the input data x_j are multiplied by weights ($w_j^{(1)}$), but the sum of all these products forms the argument of a hyperbolic tangent:

$$h = \tanh\left(\sum_j w_j^{(1)} x_j + \theta\right) \qquad \text{with} \qquad y = w^{(2)} h + \theta^{(2)} \quad (3)$$

† In this particular case, a physical model exists which proves that the dependence on concentration is not linear [4]. In general, blind models such as linear regression or neural network analysis are only used when physical models are not available or when the latter are tedious to apply.

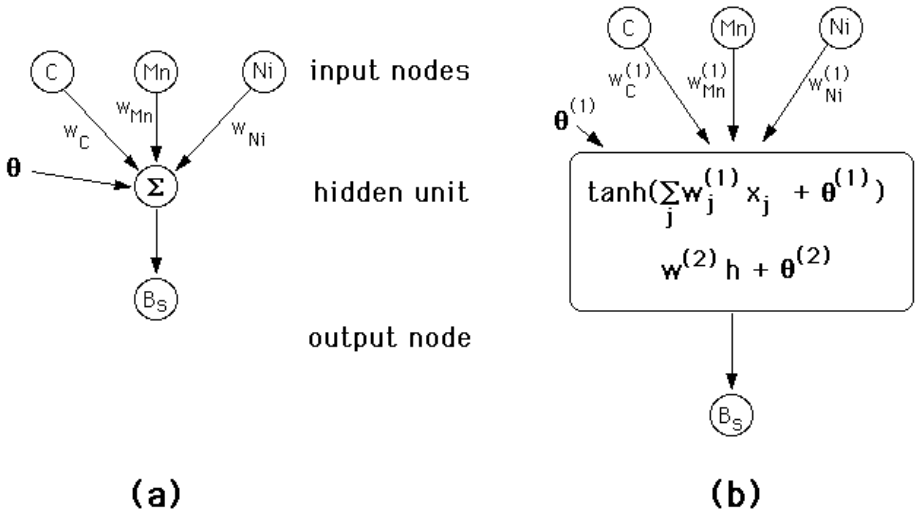

Fig. 1: (a) A neural network representation of linear regression. (b) A non–linear network representation.

where $w^{(2)}$ is a weight and $\theta^{(2)}$ another constant. The strength of the hyperbolic tangent *transfer function* is determined by the weight w_j. The output y is therefore a non–linear function of x_j, the function usually chosen being the hyperbolic tangent because of its flexibility. The exact shape of the hyperbolic tangent can be varied by altering the weights (Fig. 2a). Difficulty (c) is avoided because the hyperbolic function varies with position in the input space.

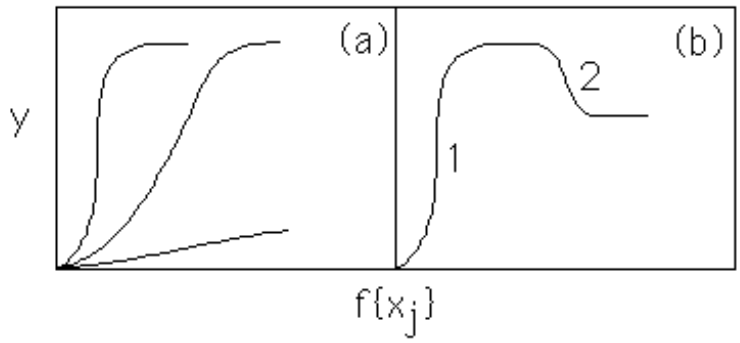

Fig. 2: (a) Three different hyperbolic tangent functions; the "strength" of each depends on the weights. (b) A combination of two hyperbolic tangents to produce a more complex model.

A one hidden-unit model may not however be sufficiently flexible. Further degrees of non–linearity can be introduced by combining several of the hyperbolic tangents (Fig. 2b), permitting the neural network method to capture almost arbitrarily non–linear relationships. The number of tanh functions per input is the number of hidden units; the structure of a two hidden unit network is shown in Fig. 3.

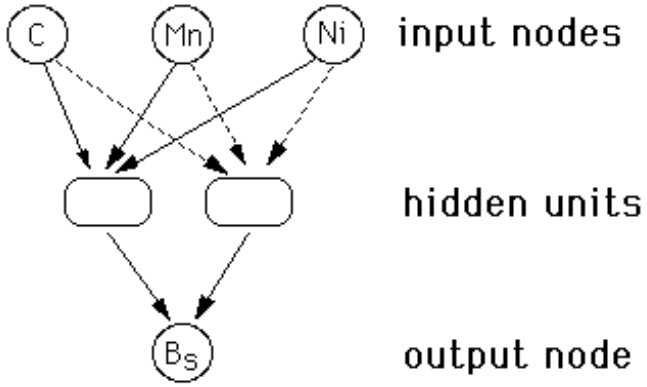

Fig. 3: The structure of a two hidden–unit neural network. Details have been omitted for simplicity.

The function for a network with i hidden units is given by

$$y = \sum_i w_i^{(2)} h_i + \theta^{(2)} \tag{4}$$

where

$$h_i = \tanh\left(\sum_j w_{ij}^{(1)} x_j + \theta_i^{(1)} \right) \tag{5}$$

Notice that the complexity of the function is related to the number of hidden units. The availability of a sufficiently complex and flexible function means that the analysis is not as restricted as in linear regression where the form of the equation has to be specified before the analysis.

The neural network can capture interactions between the inputs because the hidden units are nonlinear. The nature of these interactions is implicit in the values of the weights, but the weights may not always be easy to interpret. For example, there may exist more than just pairwise interactions, in which case the problem becomes difficult to visualise from an examination of the weights. A better method is to actually use the network to make predictions and to see how these depend on various combinations of inputs.

OVERFITTING

A potential difficulty with the use of powerful non–linear regression methods is the possibility of overfitting data. To avoid this difficulty, the experimental data can be divided into two sets, a *training* dataset and a *test* dataset. The model is produced using only the training data. The test data are then used to check that the model behaves itself when presented with previously unseen data. This is illustrated in Fig. 4 which shows three attempts at modelling noisy data for a case where y should vary with x^3. A linear model (Fig. 4a) is too simple and does not capture the real complexity in the data. An overcomplex function such as that illustrated in Fig. 4c accurately models the training data but generalises badly. The optimum model is illustrated in Fig. 4b. The training and test errors are shown schematically in Fig. 4d; not surprisingly, the training error tends to decrease continuously as the model complexity increases. It is the minimum in the test error which enables that model to be chosen which generalises best to unseen data.

This discussion of overfitting is rather brief because the problem does not simply involve the minimisation of test error. There are other parameters which control the complexity, which are adjusted automatically to try to achieve the right complexity of model [5,6].

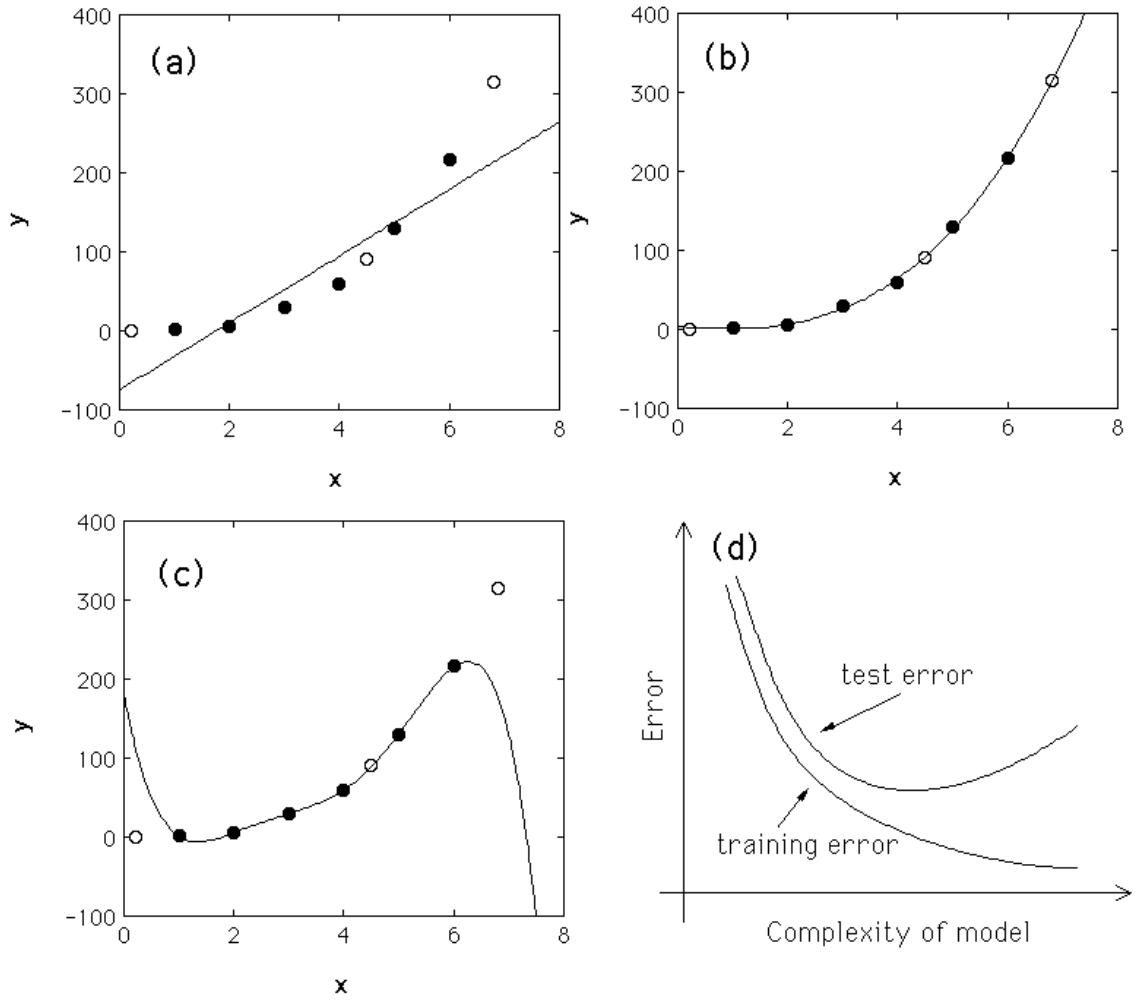

Fig. 4: Variations in the test and training errors as a function of model complexity, for noisy data in a case where y should vary with x^3. The filled points were used to create the models (*i.e.* they represent training data), and the circles constitute the test data. (a) A linear function which is too simple. (b) A cubic polynomial with optimum representation of both the training and test data. (c) A fifth order polynomial which generalises poorly. (d) Schematic illustration of the variation in the test and training errors as a function of the model complexity.

Error Estimates

The input parameters are generally assumed in the analysis to be precise and it is normal to calculate an overall error by comparing the predicted values (y_j) of the output against those measured (t_j), for example,

$$E_D \propto \sum_j (t_j - y_j)^2. \tag{6}$$

E_D is expected to increase if important input variables have been excluded from the analysis.

Whereas E_D gives an overall perceived level of noise in the output parameter, it is, on its own, an unsatisfying description of the uncertainties of prediction. Fig. 5 illustrates the problem; the practice of using the best–fit function (*i.e.* the most probable values of the weights) does not adequately describe the uncertainties in regions of the input space where data are sparse (B), or where the data are particularly noisy (A).

MacKay has developed a particularly useful treatment of neural networks in a Bayesian framework [5,6], which allows the calculation of error bars representing the uncertainty in the fitting parameters. The method recognises that there are many functions which can be fitted or extrapolated into uncertain regions of the input space, without unduly compromising the fit in adjacent regions which are rich in accurate data. Instead of calculating a unique set of weights, a probability distribution of sets of weights is used to define the fitting uncertainty. The error bars therefore become large when data are sparse or locally noisy, as illustrated in Fig. 5.

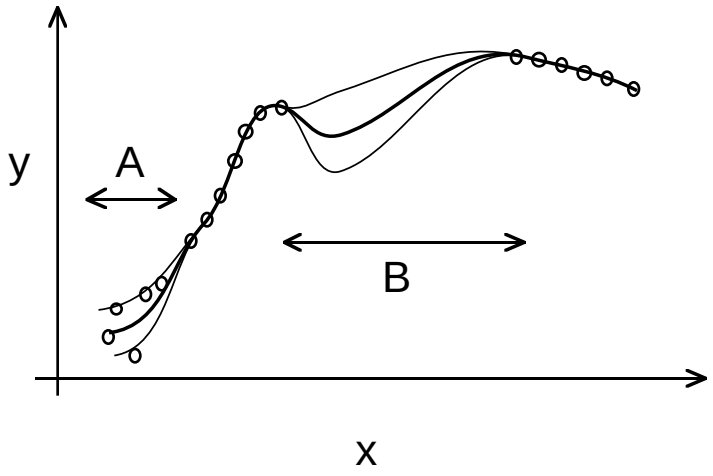

Fig. 5: Schematic illustration of the uncertainty in defining a fitting function in regions where data are sparse (B) or where they are noisy (A). The thinner lines represent error bounds due to uncertainties in determining the weights.

This methodology has proved to be extremely useful in materials science where properties need to be estimated as a function of a vast array of inputs. It is then most unlikely that the inputs are uniformly distributed in the input space.

MISCELLANY

Neural networks are often associated with the working of the human brain or with artificial intelligence. This can be misleading:

1. The neural network method described here can be expressed as an equation which is precise and which is precisely reproducible for a given set of inputs. It is a regression method of which linear regression is a subset. One has to use the considerable imagination to see in this a connection with "intelligence" or with the working of the brain.
2. The method is sometimes incorrectly described as a "black box" technique [7]. On the contrary, it is transparent, consisting of an equation and associated coefficients (the weights). Both the equation and the weights can be studied to reveal relationships and interactions.

We now proceed to discuss specific applications of neural networks in the context of materials. There are some general principles which emerge; these are emphasised in boxes.

WELDING

Welding has seen major applications of the neural network method. Examples include: weld seam tracking where the output from sensors is interpreted by a trained network to control a welding robot [8]; the interpretation of sensor information measured during welding to determine weld quality [9,10]; the detection of defects in welds using ultrasonic, radiation or other signals [11–19]; the estimation of weld profile (including penetration) from variations in welding parameters or other sensed parameters [20–27].

The use of neural networks is therefore well established in the control and monitoring of welds. We shall focus here on specific applications of greatest interest in materials science. There are other papers in the present issue of *ISIJ International*, which are not discussed here.

Charpy Toughness of Steel Weld Metal

The concept of toughness as a measure of the energy absorbed during fracture is well–developed [28,29]. It is often measured using notched–bar impact tests of which the most common is the Charpy test. A square section notched bar is fractured under specified conditions and the energy absorbed during fracture is taken as a measure of toughness. The Charpy test is empirical in that the data cannot be used directly in engineering design. It does not provide the most searching mechanical conditions. The sample has a notch, but this is less than the atomically sharp brittle crack. Although the test involves impact loading, there is a requirement to start a brittle crack from rest at the tip of the notch, suggesting that the test is optimistic in its comparison against a propagating brittle crack [29]. Most materials can be assumed to contain sub–critical cracks so that the initiation of a crack seems seldom to be an issue.

The Charpy test is nevertheless a vital quality control measure which is specified widely in international standards, and in the ranking of samples in research and development exercises. It is the most common first assessment of toughness and in this sense has a proven record of reliability. The test is usually carried out at a variety of temperatures in order to characterise the ductile–brittle transition intrinsic to body–centred cubic metals with their large Peierls barriers to dislocation motion.

The toughness of ferritic steel welds has been studied using neural networks [30]. The Charpy toughness was expressed as a function of the welding process (manual metal arc or submerged arc), the chemical composition (C, Mn, Si, Al, P, S, O & N), the test temperature and the microstructure (primary, secondary, allotriomorphic ferrite, Widmanstätten ferrite, and acicular ferrite). The inclusion of microstructure greatly limited the quantity of data available for analysis because few such results are reported in the literature. Nevertheless, the aim of the analysis was to see if the network recognised known trends in toughness as a function of the microstructure. The welding process was numerically distinguished in the analysis by using 0 and 1 for the manual and submerged arc methods.

Fig. 6 illustrates the significance (σ_w) of each of the input variables, as perceived by the neural network, in influencing the toughness of the weld. As expected, the welding–process has its own large effect; thus is well known that submerged arc welds are in general of a lower quality than manual metal arc welds. The yield strength has a major effect; it is known that an increase in the yield strength frequently leads to a deterioration in the toughness. It is also widely believed, as seen in Fig. 6, that acicular ferrite greatly influences toughness. Nitrogen has a large effect, as is well established experimentally.

A trained neural network is associated with revealing parameters other than just the transfer function and weights. For example, the extent to which each input explains variations in the output parameter can easily be examined.

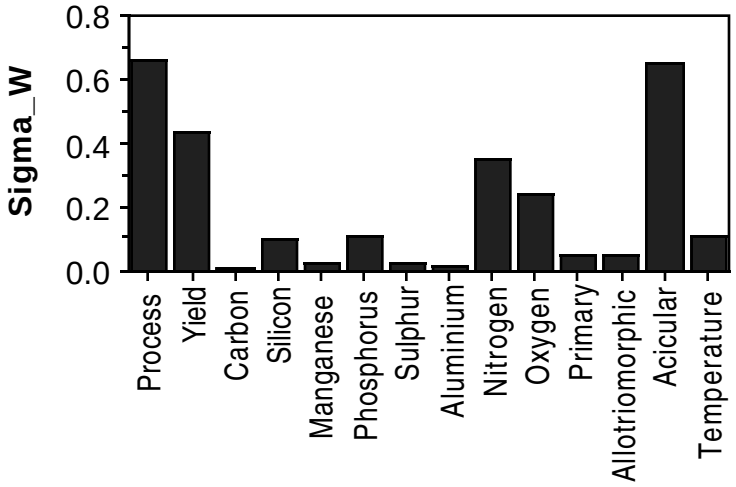

Fig. 6: Bar chart showing a measure of the model–perceived significance of each of the input variables in influencing toughness [30].

It is surprising that carbon has such a small effect (Fig. 6), but what the results really demonstrate is that the influence of carbon comes in via the strength and microstructure. Other trends have been discussed in [30].

Oxygen influences welds in both beneficial and harmful ways, *e.g.* by helping the nucleation of acicular ferrite or contributing to fracture by nucleating oxides. The predicted effect of oxygen concentration is illustrated in Fig. 7 along with the ± 1 standard deviation predicted error bars. It is clear that extrapolation into regions where data are sparse or noisy is identified with large error bars. The training data used for the toughness model had a maximum oxygen concentration of 821 parts per million.

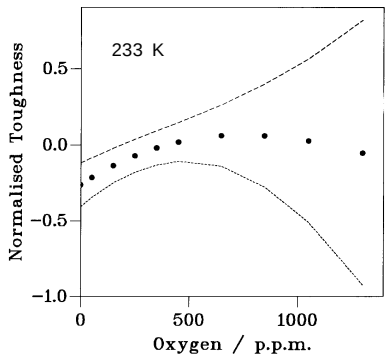

Fig. 7: Variation in the normalised toughness as a function of the oxygen concentration. Oxygen is varied here without changing any of the other inputs. The maximum oxygen concentration in the training data was 821 p.p.m.

Neural network models which indicate appropriately large error bars in regions of the input space where the fitting is uncertain are less dangerous in applications than those which simply identify a global level of noise in the output.

Fig. 8 shows how the toughness varies as a function of the manganese concentration and the test temperature. It is obvious that the effect of temperature is smaller at large concentrations of manganese, *i.e.* there is an interaction between the manganese and temperature. This interaction has been recognised naturally by the model and is expected from a metallurgical point of view [30].

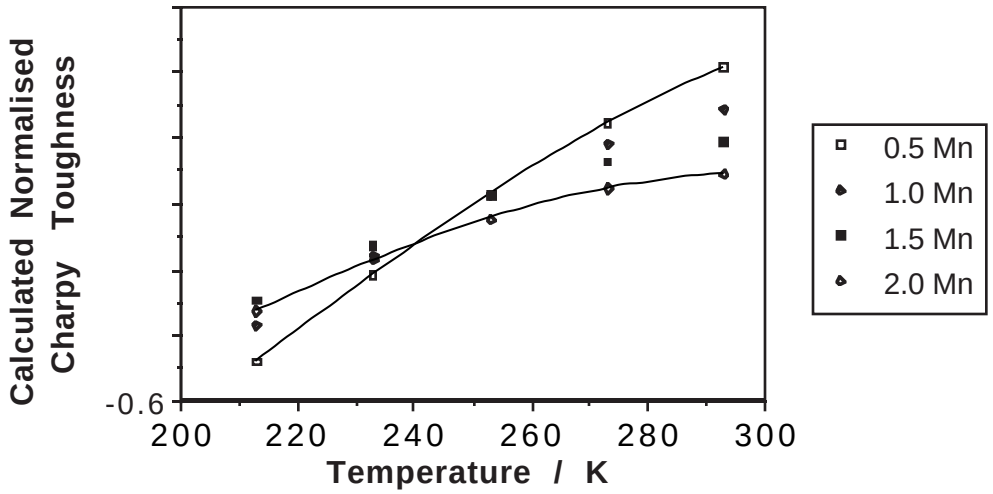

Fig. 8: Variation in the normalised toughness as a function of the manganese concentration and the test temperature.

Neural networks deduce the relationship between variables, including any interactions. In complex cases involving many variables, the interactions are revealed both qualitatively and quantitatively by examining the predictions, as illustrated in Fig. 8.

Analyses carried out without an examination of the consequences have tended to lead to the incorrect conclusion that the neural network method lacks transparency. For example, Chan *et al.* [31] created a model for the hardness of the heat affected zone of steel welds as a function of the carbon concentration, the carbon–equivalent and the cooling rate within a specified temperature range. Having produced the model, they did not continue to study how the hardness depends on each of the input parameters, whether the relationship differs for low and high carbon steels, *etc.*

The toughness model described above [30] is revealing but nevertheless, impractical for routine use because the inputs include the microstructure, which can be difficult to predict

or measure. This can be resolved by eliminating the microstructural inputs and including the welding conditions (current, voltage, speed, interpass temperature, arc efficiency) which determine the cooling rate of the weld. The microstructure is a function of the cooling rate and chemical composition (both easy to measure) so it does not have to be included explicitly.

> For practical applications, the most useful neural network models are those whose inputs are easily measured, perhaps as a part of the quality control process. On the other hand, it may be revealing to use inputs which are related directly to the output parameter, so that mechanisms are revealed.

Strength of steel welds

The tensile strength of a weld metal is frequently set higher than that of the corresponding base metal [32]. It may also be necessary to maintain a significant difference between the yield and ultimate tensile strengths in order to ensure considerable plasticity before failure, and to resist the growth of fatigue cracks. Svensson [32] has compiled an extensive list of linear regression equations for estimating the strength as a function of the weld metal chemical composition. The equations are limited to specific alloy systems and cover no more than five alloying elements. There is no facility for estimating the effect of heat treatments.

A more generally applicable neural network model has been created by Cool *et al.* [33] using data from some 1652 experiments reported in the published literature. The extensive set of variables included in the analysis is presented in Table 2, which contains information about the range of each variable. It is emphasised however, that unlike equation 1, the information in Table 2 cannot be used to define the range of applicability of the neural network model. This is because the inputs are in general expected to interact. We shall see later that it is the Bayesian framework which allows the calculation of error bars which define the range of useful applicability of the trained network.

The analysis demonstrated conclusively that there are strong interactions between the inputs; thus, the effect of molybdenum on the strength at low chromium concentrations was found to be quite different from that at high chromium concentrations. The entire dataset used in the analysis is available on the world wide web (www.msm.cam.ac.uk/map/mapmain.html). When new data are generated, these can be added to the dataset to enable the creation of more knowledgeable neural nets.

Another feature of the analysis was that Cool *et al.* used a *committee* of best models to make predictions. It is possible that a committee of models can make a more reliable prediction than an individual model [34]. The best models are ranked using the values of the test errors. Committees are then formed by combining the predictions of the best L models, where $L = 1, 2, \ldots$; the size of the committee is therefore given by the value of L. A plot of the test error of the committee versus its size L gives a minimum which defines the optimum size of the committee.

> It is good practice to use multiple good models and combine their predictions [34]. This will make little difference in the region of the input space where the fit is good, but may improve the reliability where there is great uncertainty.

Weld Cooling Rate

The time taken for a weld to cool in the temperature range 800–500 °C is an important parameter in determining the microstructure and mechanical properties of the final deposit,

Variable	Range	Mean	Standard Deviation
Carbon weight %	0.029–0.16	0.074	0.024
Silicon weight %	0.040–1.14	0.34	0.124
Manganese weight %	0.27–2.25	1.20	0.39
Sulphur weight %	0.001–0.14	0.0097	0.0069
Phosphorus weight %	0.004–0.25	0.013	0.011
Nickel weight %	0.00–3.50	0.22	0.63
Chromium weight %	0.00–9.35	0.734	2.07
Molybdenum weight %	0.00–1.50	0.17	0.35
Vanadium weight %	0.00–0.24	0.018	0.049
Copper weight %	0.00–1.63	0.074	0.224
Cobalt weight %	0.00–2.80	0.011	0.147
Tungsten weight %	0.00–2.99	0.0115	0.146
Titanium p. p. m. w.	0–690	40.86	79.9
Boron p. p. m. w.	0–69	1.17	5.78
Niobium p. p. m. w.	0–1000	57.4	151
Oxygen p. p. m. w.	132–1650	441	152
Heat Input kJ mm^{-1}	0.6–7.9	1.85	1.47
Interpass Temperature $^{\circ}C$	20–300	207.7	48.93
Tempering Temperature $^{\circ}C$	0–760	320.4	257
Tempering Time hours	0–24	5.72	6.29
Yield Strength MPa	315–920	507.3	92.8
Ultimate Tensile Strength MPa	447–1151	599	92

Table 2: The variables used in the analysis of strength. The abbreviation p. p. m. w. stands for parts per million by weight. Notice that this table cannot be used to define the range over which a neural network might be expected to give safe predictions.

and indeed of the adjacent heat–affected zone. An analytical approximation to the heat flow problem [35,36] has indicated that the time should depend on the heat input (*i.e.* welding current, voltage, speed and arc transfer efficiency), the substrate temperature and the thickness of the plate (*i.e.* the dimensionality of the heat flow). Separate equations are required for 2, 3 or $2\frac{1}{2}$ dimensional heat flow.

Chan *et al.* [37] used the inputs indicated by Adams physical–model and incorporated them into a neural network model, to obtain a single model for all dimensionalities of heat flow. They demonstrated that the accuracy achieved is better with the neural network, given the approximations inherent in the analytical equations of Adam's theory.

One difficulty is that the neural network model used does not give errors bars which are dependent on the local fit so that the actual range of applicability of the model is not clear. The reliability of the model is not established when extrapolated or interpolated beyond the domain of the training dataset.

When comparing neural network models with physical models, it is useful to illustrate and study the behaviour of the neural network models in domains beyond the range of the training data.

Hot Cracking of Welds

Solidification cracking occurs in welds during cooling from the liquidus temperature, if the density changes associated with solidification and thermal contraction cannot be accommodated by fluid flow or by the motion of the solid components which constitute the weld assembly. Hot–cracking tests frequently lead to a discrete outcome, *i.e.* whether cracking occurs or not. Such a problem is known as a binary classification problem, and a *classification* neural network is used to model the probability of a crack as a function of the input variables [34]. A probability of 1 represents definite cracking whereas a probability of 0 represents the absence of cracking. In the Bayesian framework the uncertainty of the prediction is accounted for by a process of *marginalisation*. The effect of marginalisation is to take the output of the best fit neural network and move it closer to a probability of 0.5 by an amount depending on the parameters' uncertainty. The value 0.5 in the output represents the highest level of uncertainty.

An application of the classification neural network to the hot–cracking of ferritic steel welds is shown in Fig. 9 [38].

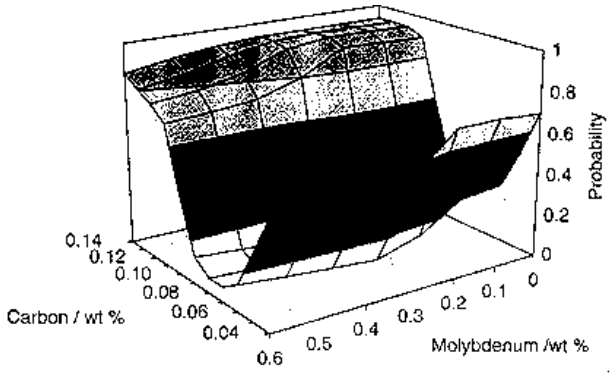

Fig. 9: Predicted effect of molybdenum and carbon on solidification cracking in steel welds [38].

SUPERALLOYS

Overall Strength

The yield and ultimate tensile strength of nickel–base superalloys with γ/γ' microstructures has been modelled [39,40] using the neural network method, as a function of the Ni, Cr, Co, Mo, W, Ta, Nb, Al, Ti, Fe, Mn, Si, C, B, and Zr concentrations, and of the test temperature. The analysis is based on data selected from the published literature. The trained models were subjected to a variety of metallurgical tests. As expected, the test temperature (in the range 25–1100 °C) was found to be the most significant variable influencing the tensile properties, both via the temperature dependence of strengthening mechanisms and due to

variations in the γ' fraction with temperature. Since precipitation hardening is a dominant strengthening mechanism, it was encouraging that the network recognised Ti, Al and Nb to be key factors controlling the strength. The physical significance of the neural network was apparent in all the interrogations performed.

One example illustrating this last point is presented in Fig. 10. The softening of the γ matrix is offset by the remarkable reversible increase in the strength of the γ' with increasing temperature.

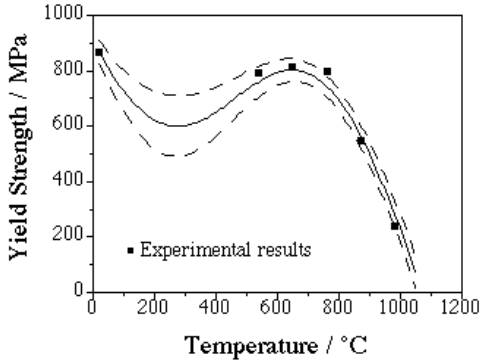

Fig. 10: Predicted temperature dependence of the yield strength of a γ/γ' superalloy (after Tancret, private communication).

A further revelation from the neural network analysis came from the error estimates, which demonstrated clearly that there are great uncertainties in the experimental data on the effect of large concentrations of molybdenum on the tensile properties. This has identified a region where careful experiments are needed; molybdenum is known to have a large influence on the γ/γ' lattice misfit.

FATIGUE PROPERTIES

Fatigue is one of the most difficult mechanical properties to predict. An extensive literature review has been carried out to assess methods for predicting the fatigue crack growth rates [41]. This included an examination of physical models, which where either found to lack generality or to give only qualitative indications of the trends [41,42]. Experiments on the initiation and propagation of cracks in turbine–disc superalloys have failed to clarify how fatigue theory could be used to make quantitative predictions.

A neural network method has therefore been used after identifying some 51 variables that could be expected to influence the fatigue crack growth rate in nickel base superalloys [43]. In fact, it is not difficult to compile an even larger list of variables which could influence fatigue properties, but an over ambitious choice of inputs is likely to reduce the number of data available in the literature.

The number of inputs chosen is a compromise between the definition of the problem and the availability of data. The neural network method cannot cope with missing values. An over ambitious choice of input variables will in general limit the number of complete sets of data available for analysis. On the other hand, neglect of an important variable will lead to an increase in the noise associated with predictions.

The variables studied included the stress intensity range ΔK, $\log\{\Delta K\}$ chemical composition, temperature, grain size, heat treatment, frequency, load waveform, atmosphere, R–ratio, the distinction between short and long crack growth, sample thickness and yield strength. The analysis was conducted on some 1894 data collected from the published literature. The reason for including both ΔK and $\log\{\Delta K\}$ as inputs is because the latter has metallurgical significance since a plot of the logarithm of the crack growth rate versus $\log\{\Delta K\}$ is a simple and well–established relationship. However, there may exist unknown and separate effects of ΔK, in which case that should be included as an additional input. It is encouraging that the trained network in fact assigned the greatest significance to $\log\{\Delta K\}$.

If a certain functional relationship is expected between the raw output and a particular input, than that input can be included twice, in its functional form and in its raw form. The inclusion of the latter prevents bias.

The model, unlike any experimental approach, could be used to study the effect of each variable in isolation. This gave interesting results. For example, it was verified that an increase in the grain size should lead to a decrease in the fatigue crack growth rate, when the grain size is varied without affecting any other input. This cannot be done in experiments because the change in grain size is achieved by altering the heat treatment, which in turn influences other features of the microstructure (Fig. 11). It was also possible to confirm that $\log\{\Delta K\}$ is more strongly linked to the fatigue crack growth rate than to ΔK, as expected from the Paris law. There are many other metallurgical trends revealed [43].

The neural network model can in principle be used to examine the effect of an individual input on the output parameter, whereas this may be incredibly difficult to do experimentally.

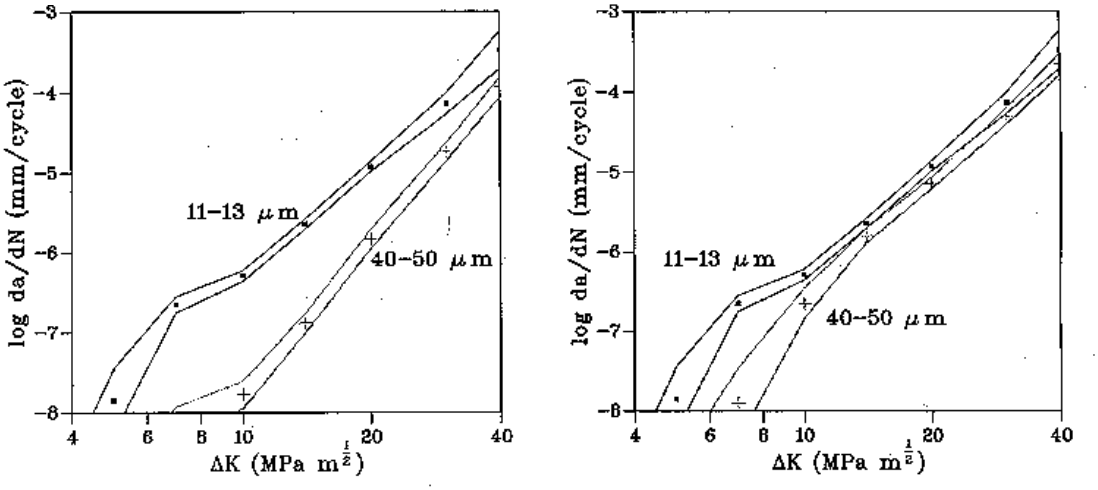

Fig. 11: Astroloy: (a) effect of grain size alone; (b) effect of heat treatment alone [43].

In another approach [44] a different neural computing approach was used to focus on stage II of the Paris regime, where the growth rate should depend mainly on the stress intensity range, Young's modulus and yield strength. The model was used successfully in estimating new test data. The effect of the ultimate tensile strength and phase stability was also investigated; although this proved promising, it is probable that the results will be more convincing when a greater range of data become available.

Fatigue Threshold

In a recent study of the fatigue thresholds in nickel–base superalloys, Schooling *et al.* have attempted to compare a "neurofuzzy" modelling approach with the classical neural network [7]. The application of fuzzy rules to the network involves the biassing of the inputs according to human experience.

It was suggested that the fuzzy method has an advantage with restricted datasets because the complexity of the relationships can be restricted by the operator. This conclusion is surprising because the complexity of a classical neural network, when assessed for generalisation, naturally tends to be minimised for small datasets.

Schooling *et al.* found it necessary to make significant adjustments to the fuzzy rules in order reduce the mean square error to a value comparable to the classical network. It is evident that there is considerable operator bias introduced in designing fuzzy networks. This may not be satisfactory for complex problems where the actual relationships are not understood to begin with.

The comparison of the two methods by Schooling *et al.* does not seem justified because the predictions of the neurofuzzy method were not accompanied by error bars (other than the mean square error).

Creep of Superalloys

The creep rupture life of nickel base superalloys has been modelled as a function of 42 variables including Cr, Co, C, Si, Mn, P, S, Mo, Cu, Ti, Al, B, N, Nb, Ta, Zr, Fe, W, V, Hf, Re, Mg, La and ThO_2 [45]. Other variables include four heat treatment steps (characterised by temperature, duration and cooling rate), the sample shape and the solidification method.

Sathyanarayanan *et al.* [46] have developed a neural network model for the "creep feed grinding" of nickel–base superalloys and titanium alloys, using the feed rate, depth of cut and wheel bond type as inputs, and the surface finish, force and power as outputs.

Lattice Parameters of Superalloys

The lattice constants of the γ and γ' phases of nickel superalloys have been modelled using a neural network within a Bayesian framework [47]. The analysis was based on new X–ray measurements and peak separation techniques, for a number of alloys and as a function of temperature. These data were supplemented using the published literature.

The lattice parameters of the two phases were expressed as a non–linear function of eighteen variables including the chemical composition and temperature. It was possible to estimate the uncertainties and the method has proved to be extremely useful in understanding both the effect of solutes on the lattice mismatch, and on how this mismatch changes with temperature.

TRANSFORMATIONS

Martensite–Start Temperature

Martensite forms without diffusion and has a well–defined start–temperature (M_S), which for the majority of engineering steels is only sensitive to the chemical composition of the austenite. There are numerous regression equations in the published literature, which have been used for many decades in the estimation of M_S, mostly as a linear function of the chemical composition. Vermeulen *et al.*[48] demonstrated that a neural network model can do this much

more effectively, and at the same time demonstrated clear interactions between the elements. For example, the magnitude of the effect of a given carbon content on M_S is much larger at low manganese levels than at high manganese concentrations. This is in contrast to all published equations where the sensitivity to carbon is independent of the presence of other alloying elements.

Continuous Cooling Transformation Diagrams

The transformation of austenite as the temperature decreases during continuous cooling has been modelled with the neural network method using the chemical composition, the austenitisation temperature and cooling rate as inputs [49]. The results were concluded to be satisfactory but with large errors particularly for the bainite reaction. These large errors were attributed partly to noise in the experimental data, to the neglect of austenite grain size as an input, and to the assumption that all transformations occur at all cooling rates, whereas this is not the case in practice.

The network is empirical and hence permits a calculation of each transformation under all circumstances, even when this involves extrapolation into forbidden domains. This difficulty might be avoided by modelling the total fraction of transformation and the transformation–start temperatures separately, and then using a logical rule to determine whether the transformation is real or not.

A further effect is illustrated by a later study [50]; the neural network calculations of CCT curves as illustrated in Fig. 12 appear jagged, rather than the expected smooth curves. This is because the points on the curve are calculated individually and have been joined without accounting for errors. If smooth curves are definitely required, then the experimental curves should be represented mathematically, and the parameters required to describe these curves can be used as inputs. There will, of course, be error bars to be taken into account but these will be smoothly disposed about the most expected curve.

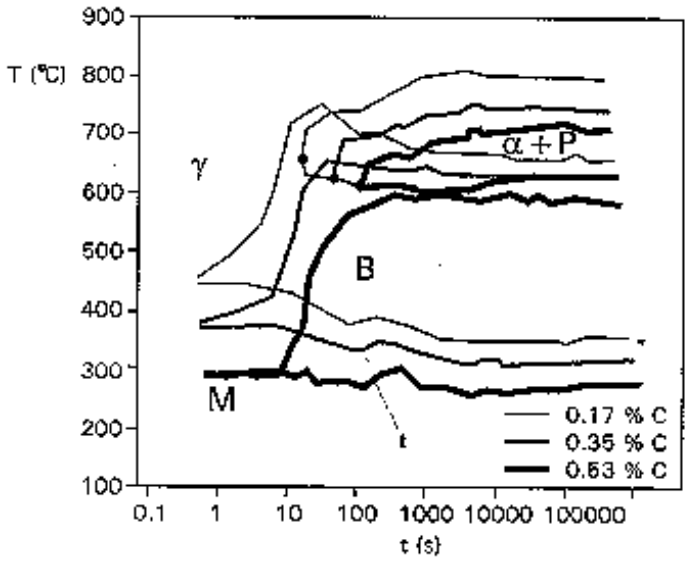

Fig. 12: The effect of carbon on the CCT diagram of an alloy steel as a function of the carbon concentration [50].

Austenite Formation

Most commercial processes rely to some extent on heat treatments which cause the steel

to revert into the austenitic condition. This includes the processes involved in the manufacture of wrought steels, and in the fabrication of steel components by welding.

The formation of austenite during heating differs in many ways from those transformations that occur during the cooling of austenite. Both the diffusion coefficient and the driving force increase with the extent of superheat above the equilibrium temperature, so that the rate of austenite formation must increase indefinitely with temperature.

There is another important difference between the transformation of austenite, and the transformation to austenite. In the former case, the kinetics of transformation can be described completely in terms of the alloy composition and the austenite grain size. By contrast, the microstructure from which austenite may grow can be infinitely varied. Many more variables are therefore needed to describe the kinetics of austenite formation.

Gavard *et al.* [51] have created a neural network model in which the Ac_1 and Ac_3 temperatures of steel are estimated as a function of the chemical composition and the heating rate. The model has been very revealing; some of the features are illustrated in Fig. 13. As might be expected, the Ac_1 temperature decreases with carbon concentration reaching a limiting value which is very close to the eutectoid temperature of about 723 °C. This latter limit is expected because of the slow heating rate and the fact that the test steel does not contain any substitutional solutes. Note that there is a slight underprediction of the Ac_1 temperature for pure iron, although the expected temperature of about 910 °C is within the 95% confidence limits of the prediction (twice the width of the error limits illustrated in Fig. 13).

By contrast, the Ac_3 temperature appears to go through a minimum at about the eutectoid carbon concentration. This is also expected because the Ae_3 temperature also goes through a minimum at the eutectoid composition. Furthermore, unlike the Ac_1 temperature, the minimum value of the calculated Ac_3 never reaches the eutectoid temperature; even at the slow heating rate it is expected that the austenite transformation finishes at some superheat above the eutectoid temperature, the superheat being reasonably predicted to be about 25 °C.

At slow heating rates, the predicted Ac_1 and Ac_3 temperatures are in fact very close to the equilibrium Ae_1 and Ae_3 temperatures and insensitive to the rate of heating. As expected, they both increase more rapidly when the heating rate rises exceeds about $10\,^{\circ}\mathrm{C\,s^{-1}}$. The significant maximum as a function of the heating rate is unexpected and is a prediction which suggest that further experiments are necessary.

Neural network analysis of published data can help identify experiments in two ways. First, unexpected trends might emerge. Secondly, the error bars may be so large as to make the prediction uncertain, in which case experiments are necessary.

STEEL PROCESSING & MECHANICAL PROPERTIES

Hot Rolling

The properties of steel are greatly enhanced by the rolling process. It is possible to cast steel into virtually the final shape but such a product will not have the quality or excellence of a carefully rolled product.

Singh *et al.* [52] have developed a neural network model in which the yield and tensile strength of the steel is estimated as a function of some 108 variables, including the chemical composition and an array of rolling parameters. Implicit in the rolling parameters is the thermal history and mechanical reduction of the slab as it progresses to the final product. The training data comes from sensors on the rolling mill. There is therefore no shortage of data, the limitation in this case being the need to economise on computations. There are some

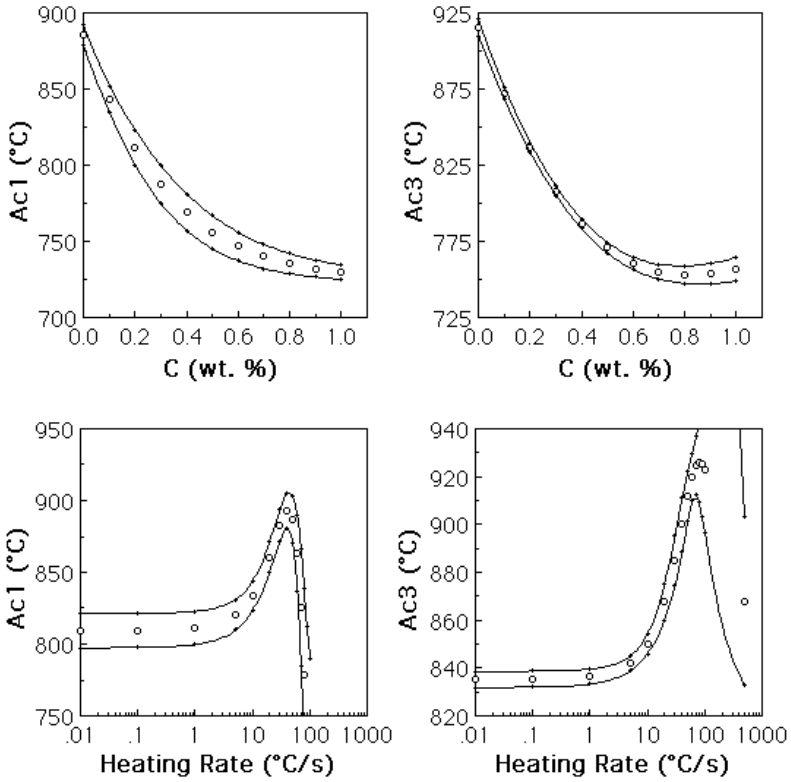

Fig. 13: (a,b) The predicted variation in the Ac_1 and Ac_3 temperatures of plain carbon steels as a function of the carbon concentration at a heating rate of $1\,^{\circ}C\,s^{-1}$. (c,d) The predicted variation in the Ac_1 and Ac_3 temperatures of an Fe–0.2 wt% alloy as a function of the heating rate. In all of these diagrams, the lines represent the $\pm 1\sigma$ error bars about the calculated points. All the results presented here are based on models with four and two hidden units for the Ac_1 and Ac_3 temperatures respectively.

exciting results which make sense from a metallurgical point of view, together with some novel predictions on a way to control the yield to tensile strength ratio. A similar model by Korczak *et al.* [53] uses microstructural parameters as inputs and has been applied to the calculation of the ferrite grain size and property distribution through the thickness of the final plate.

Vermeulen *et al.* [54] have similarly modelled the temperature of the steel at the last finishing stand. They demonstrated that it is definitely necessary to use a non–linear representation of the input variables to obtain an accurate prediction of the temperature. The control of strip temperature on a hot strip mill runout table has also been modelled by Loney *et al.* [55].

Heat Treatment

A Jominy test is used to measure the hardenability of steel during heat treatment. Vermeulen *et al.* [56] have been able to accurately represent the Jominy hardness profiles of steels as a function of the chemical composition and austenitising temperature.

Mechanical Properties

There are many other examples of the use of neural networks to describe the mechanical properties of steels; Dumortier *et al.* have modelled the properties of microalloyed steels [57]; Mllykoski [58,59] has addressed the problem of strength variations in thin steel sheets;

microstructure–property relationships of C–Mn steels [60]; the tensile properties of mechanically alloyed iron [61,62] with a comparison with predictions using physical models; the hot–torsion properties of austenite [63].

POLYMERIC & INORGANIC COMPOUNDS

Neural network methods have been used to model the glass transition temperatures of amorphous and semi–crystalline polymers to an accuracy of about 10 K, and similar models have been developed for relaxation temperatures, degradation temperature, refractive index, tensile strength, elongation, notch strength, hardness, *etc.* [64–66]. The molecular structure of the monomeric repeating unit is described using topological indices from graph theory. The techniques have been exploited, for example, in the design of polycarbonates for increased impact resistance. In another analysis, the glass transition temperature of linear homopolymers has been expressed as a function of the monomer structure, and the model has been shown to generalise to unseen data to an accuracy of about 35 K [67].

Comparison with Quantum Mechanical Calculations

There is an interesting study [68] which claims that neural networks are able to predict the equilibrium bond length, bond dissociation energy and equilibrium stretching frequency more accurately, and far more rapidly than quantum mechanical calculations. The work dealt with diatomic molecules such as LiBr, using thirteen inputs: atomic number, atomic weight (to include isotope effects), valence electron configuration (s, p, d, f electrons) for both atoms, and the overall charge. The corresponding quantum mechanical calculations used effective core potentials as inputs. It was found that all three molecular properties could be predicted more accurately using neural networks, with a considerable reduction in the computational effort.

Such a comparison of a physical model with one which is empirical is not always likely to be fair. In general, an appropriate neural network model should perform badly when compared with a physical model, when both are presented with precisely identical data. This is because the neural network can only learn from the data it is exposed to. By contrast, the physical model will contain relationships which have some justification in science, and which impose constraints on the behaviour of the model during extrapolation. As a consequence, the neural network is likely to violate physical principles when used without restriction. The continuous cooling transformation curve model discussed above [49,50] is an example where the neural network produces information in forbidden domains and produces jagged curves, which a physical model using the same data would not because the form of the curves would be based on phase transformation theory [*e.g.* 69].

CERAMICS

Ceramic Matrix Composites

Ceramic matrix composites rely on a weak interface between the matrix and fibre. This introduces slip and debonding during deformation, thus avoiding the catastrophic propagation of failure. The mathematical treatment of the deformation has a large number of variables with many fitting parameters. For an Al_2O_3 matrix SiC whisker composite a constitutive law has been derived using an artificial neural network, using inputs generated by finite element analysis [70].

Hybrid models can be created by training neural networks on data generated by physical models.

There are many examples where neural networks have been used to estimate machine–tool wear. For example, Ezuguwu *et al.* [71] have modelled the tool life of a mixed–oxide ceramic cutting tool as a function of the feed rate, cutting speed and depth of cut. Tribology issues in machining, including the use of neural networks, have been reviewed by Jahanmir [72].

Neural networks are also used routinely in the control of cast ceramic products made using the slip casting technique, using variables such as the ambient conditions, raw material information and production line settings [73]. In another application, scanning electron microscope images of ceramic powders were digitised and processed to obtain the particle boundary profile; this information was then classified using a neural approach, with exceptionally good results even on unseen data [74].

THIN FILMS & SUPERCONDUCTORS

A lot of the materials science type issues about thin films naturally involve deposition and characterisation. The deposition process can be very complicated to control and is ideally suited for neural network applications.

Neural networks have been used to interpret Raman spectroscopy data to deduce the superconducting transition temperature of YBCO thin films during the deposition process [75]; to characterise reflection high–energy electron diffraction patterns from semiconductor thin films in order to monitor the deposition process [76]; to rapidly estimate the optical constants of thin films using the computational results of a physical model of thin films [77]; and there are numerous other similar examples.

There is one particular application which falls in the category of "alloy design"; Asada *et al.* [78] trained a neural network on a database of $(Y_{1-x}Ca_x)Ba_2Cu_3O_z$ and $Y(Ba_{2-x}Ca_x)Cu_3O_z$, where z is generally less than 7, the ideal number of oxygen atoms. The output parameter was the superconducting transition temperature as a function of x and z. They were thus able to predict the transition temperature of $YBa_2Cu_3O_z$ doped with calcium. It was demonstrated that the highest temperature is expected for $x = 0.3$ and $z = 6.5$ in $(Y_{1-x}Ca_x)Ba_2Cu_3O_z$ whereas a different behaviour occurs for $Y(Ba_{2-x}Ca_x)Cu_3O_z$.

COMPOSITES

There are many applications where vibration information can be used to assess the damage in composite structures [*e.g.* 79–81]. Acoustic emission signals have been used to train a neural network to determine the burst pressure of fiberglass epoxy pressure vessels [82]. There has even been an application in the detection of cracks in eggs [83].

One different application is in the optimisation of the curing process for polymer–matrix composites made using thermosetting resins [84]. An interesting application is the modelling of damage evolution during forging of Al–SiC particle reinforced brake discs [85]. The authors were able to predict damage in a brake component previously unseen by the neural network model.

Hwang *et al.* [86] compared a prediction of the failure strength of carbon fibre reinforced polymer composite, made using a neural network model, against the Tsai–Wu theory and an alternative hybrid model. Of the three models, the neural network gave the smallest root–mean square error. Nevertheless, the earlier comments about the validity of the neural network in extrapolation *etc.* remain as a cautionary note in comparisons of neural and physical models.

PUBLICATION

The application of neural networks in materials science is a rapidly growing field. There are numerous papers being published but the vast majority are of little use other than to the authors. This is because the publications almost never include detailed algorithms, weights

and databases of the kind necessary to reproduce the work. Work which cannot be reproduced or checked goes against the principles of scientific publication.

The minimum information required to reproduce a trained network is the structure of the network, the nature of the transfer functions, the weights corresponding to the optimised network and the range of each input and output variable. Such detailed numerical information is unlikely to be accepted for publication in journals. There is now a world wide web site where this information can be logged for common access:

www.msm.cam.ac.uk/map/mapmain.html

It is also good practice to deposit the datasets used in the development of neural networks in this materials algorithms library [87].

SUMMARY

Neural networks are clearly extremely useful in recognising patterns in complex data. The resulting quantitative models are transparent; they can be interrogated to reveal the patterns and the model parameters can be studied to illuminate the significance of particular variables. A trained network embodies the knowledge within the training dataset, and can be adapted as knowledge is accumulated.

Neural network analysis has had a liberating effect on materials science, by enabling the study of incredibly diverse phenomena which are not as yet accessible to physical modelling. The methodology is used extensively in process control, process design and alloy design. It is a technique which should now form a standard part of the undergraduate curriculum.

Acknowledgments

I am immensely grateful to David MacKay for his help and friendship over many years, and to Franck Tancret for reviewing the draft manuscript. I would also like to thank Dr Kaneaki Tsuzaki and the editorial board of ISIJ International for inviting us to assemble a special issue on neural networks.

REFERENCES

1. J. S. Bowles and J. K. MacKenzie: *Acta Metallurgica,* **2** (1954) 129–137.
2. M. S. Wechsler, D. S. Lieberman and T. A. Read: *Trans. Amer. Inst. Min. Metall. Engrs.,* **197** (1953) 1503–1515.
3. W. Stevens and A. J. Haynes: *Journal of The Iron and Steel Institute,* **183** (1956) 349–359.
4. H. K. D. H. Bhadeshia: *Acta Metallurgica,* **29** (1981) 1117–1130.

5 D. J. C. MacKay: *Neural Computation,* **4** (1992) 415–447.

6 D. J. C. MacKay: *Neural Computation,* **4** (1992) 448–472.

7 J. M. Schooling, M. Brown and P. A. S. Reed: *Materials Science and Engineering A,* **A260** (1999) 222-239.

8. S. H. Nam and S. V. Oh: *Applied Intelligence,* **10** (1999) 53–70.
9. D. C. Lim and D. G. Gweon: *Journal of Engineering Manufacture,* **213** (1999) 51–57.
10. T. K. Meng and C. Butler: *International Journal of Advanced Manufacturing Technology,* **13** (1997) 666–675.
11. W. Yi and I. S. Yun: *KSME International Journal,* **12** (1998) 1150–1161.
12. R. Polikar, L. Udpa, S. S. Udpa and T. Taylor: *IEEE Trans. on Ultrasonics, Ferroelectrics and Frequency Control,* **45** (1998) 614–625.
13. T. W. Liao and K. Tang: *Applied Artificial Intelligence,* **11** (1997) 197–218.
14. A. Masnata and M. Sunseri: *NDT & E International,* **29** (1996) 87–93.
15. D. Farson and J. Kern: *Lasers in Engineering,* **4** (1995) 13–23.
16. L. M. Brown and R. Denale: *Naval Engineers Journal,* **107** (1995) 179–190.
17. A. McNab and I. Dunlop: *Insight,* **37** (1995) 11–16.
18. E. V. Hill, P. L. Israel and G. L. Knotts: *Materials Evaluation,* **51** (1993) 1040.
19. C. G. Winsdor, F. Anselme, L. Capineri and J. P. Mason: *British Journal of Non–Destructive Testing,* **35** (1993) 15–22.
20. J. D. Brown, M. G. Rodd and N. T. Williams: *Ironmaking and Steelmaking,* **25** (1998) 199–204.
21. S. C. Juang, Y. S. Tarng and H. R. Lii: *Journal of Materials Processing Technology,* **75** (1998) 54–62.
22. P. Li, M. T. C. Fang and J. Lucas: *Journal of Materials Processing Technology,* **71** (1997) 288–298.
23. Y. M. Zhang, L. Li and R. Kovacevic: *Journal of Manufacturing Science and Engineering – Transactions of ASME,* **119** (1997) 631–643.
24. H. S. Moon and S. J. Na: *Journal of Manufacturing Systems,* **15** (1996) 392–403.
25. R. Kovacevic, Y. M. Zhang and L. Li: *Welding Journal,* **75** (1996) S317–S329.
26. D. Farson, K. Hillsley, J. Sames and R. Young: *Journal of Laser Applications,* **8** (1996) 33–42.
27. Y. M. Zhang, R. Kovacevic and L. Li: *International Journal of Machine Tools & Manufacture,* **36** (1996) 799–816.
28. J. F. Knott: *Fundamentals of Fracture Mechanics,* Butterworths, London (1973)
29. A. H. Cottrell: *International Journal of Pressure Vessels and Piping,* **64** (1995) 171–174.
30. H. K. D. H. Bhadeshia, D. J. C. MacKay and L.–E. Svensson: *Materials Science and Technology,* **11** (1995) 1046–1051.
31. B. Chan, M. Bibby and N. Holtz: *Canadian Metallurgical Quarterly,* **34** (1995) 353–356.
32. L.–E. Svensson: *Control of Microstructure and Properties in Steel Arc Welds,* CRC Press, London, (1994)
33. T. Cool, H. K. D. H. Bhadeshia and D. J. C. MacKay: *Materials Science and Engineering A,* **223** (1997) 179–185.

34. D. J. C. MacKay: *Mathematical Modelling of Weld Phenomena III,* eds H. Cerjak and H. K. D. H. Bhadeshia, The Institute of Materials, London, (1997) 359–389.
35. C. M. Adams, Jr.: *Welding Journal,* **37** (1958) S210–S215.
36. P. Jhaveri, W. G. Moffat and C. M. Adams, Jr.: *Welding Journal,* **42** (1962) 12.
37. B. Chan, M. Bibby and N. Holtz: *Transactions of the Canadian Society of Mechanical Engineers (CSME),* **20** (1996) 75–86.
38. K. Ichikawa, H. K. D. H. Bhadeshia and D. J. C. MacKay: *Science and Technology of Welding and Joining,* **1** (1996) 43-50.
39 J. Jones and D. J. C. MacKay: *8th Int. Symposium on Superalloys,* Seven Springs, Pennsylvania, USA, September '96, eds R. D. Kissinger *et al.*, published by TMS, (1996) 417–424.
40 J. Jones, D. J. C. MacKay and H. K. D. H. Bhadeshia: *Proc. 4th International Symposium on Advanced Materials,*eds Anwar ul Haq *et al.*, A. Q. Kahn Research Laboratories, Pakistan (1995) 659–666.
41 J. M. Schooling: *The modelling of fatigue in nickel base alloys,* Ph.D. Thesis, University of Cambridge (1997)
42 J. M. Schooling and P. A. S. Reed: *8th Int. Symposium on Superalloys,* Seven Springs, Pennsylvania, USA, September '96, eds R. D. Kissinger *et al.*, published by TMS (1996) 409–416.
43 H. Fujii, D. J. C. MacKay and H. K. D. H. Bhadeshia: *ISIJ International,* **36** (1996) 1373–1382.
44 J. M. Schooling and P. A. S. Reed: *Proc. 4th International Symposium on Advanced Materials,* eds Anwar ul Haq *et al.*, A. Q. Kahn Research Laboratories, Pakistan (1995) 555–561.
45 H. Fujii, D. J. C. MacKay, H. K. D. H. Bhadeshia, H. Harada and K. Nogi: *6th Leige Conference, Materials for Advanced Power Engineering,* October 1998, Leige, Belgium, (1998) 1401–1410.
46 G. Sathyanarayanan, I. J. Lin and M. K. Chen: *International Journal of Production Research,* **30** (1992) 2421–2438.
47 S. Yoshitake, V. Narayan, H. Harada, H. K. D. H. Bhadeshia and D. J. C. MacKay: *ISIJ International,* **38** (1998) 495–502.
48 W. G. Vermeulen, P. F. Morris, A. P. de Weijer and S. van der Zwaag: *Ironmaking and Steelmaking,* **23** (1996) 433–437.
49 W. G. Vermeulen, S. van der Zwaag, P. F. Morris and T. de Weijer: *Steel Research,* **68** (1997) 72–79.
50 P. J. van der Wolk, C. Dorrepaal, J. Sietsma and S. van der Zwaag: *Intelligent Processing of High Performance Materials,* Research and Technology Organization, Neuilly-sur-seine, France, (1998) 6–1 to 6–6.
51 L. Gavard, H. K. D. H. Bhadeshia, D. J. C. MacKay and S. Suzuki: *Materials Science and Technology,* **12** (1996) 453–463.
52 S. B. Singh, H. K. D. H. Bhadeshia, D. J. C. MacKay, H. Carey and I. Martin: *Ironmaking and Steelmaking,* **25** (1998) 355–365.
53 P. Korczak, H. Dyja and E. Labuda: *Journal of Materials Processing Technology,* **80–1** (1998) 481–486.
54 W. G. Vermeulen, A. Bodin and S. van der Zwaag: *Steel Research,* **68** (1997) 20–26.
55 D. Loney, I. Roberts and J. Watson: *Ironmaking and Steelmaking,* **24** (1997) 34–49.
56 W. G. Vermeulen, P. J. van der Wolk, A. P. de Weijer and S. van der Zwaag: *Journal of Materials Engineering and Performance,* **5** (1996) 57–63.
57 C. Dumortier, P. Lehert, P. Krupa and A. Charlier: *Materials Science Forum,* **284** (1998) 393–400.
58 P. Myllykoski: *Journal of Materials Processing Technology,* **79** (1998) 9–13.

59 P. Myllykoski, J. Larkiola and J. Nylander: *Journal of Materials Processing Technology,* **60** (1996) 399–404.
60 Z. Y. Liu, W. D. Wang and W. Gao: *Journal of Materials Processing Technology,* **57** (1996) 332–336.
61 A. Y. Badmos, H. K. D. H. Bhadeshia and D. J. C. MacKay: *Materials Science and Technology,* **14** (1998) 793–809.
62 A. Y. Badmos and H. K. D. H. Bhadeshia: *Materials Science and Technology,* **14** (1998) 1221–1226.
63 V. Narayan, R. Abad–Lera, B. Lopez, H. K. D. H. Bhadeshia and D. J. C. MacKay: *ISIJ International,* (1998) in press.
64 C. W. Ulmer, D. A. Smith, B. G. Sumpter and D. I. Noid: *Computational and Theoretical Polymer Science,* **8** (1998) 311–321.
65 B. G. Sumpter and D. W. Noid: *Journal of Thermal Analysis,* **46** (1996) 833–851.
66 B. G. Sumpter and D. W. Noid: *Macromolecular Theory and Simulations,* **3** (1994) 363–378.
67 S. J. Joyce, D. J. Osguthorpe, J. A. Padgett and G. J. Price: *Journal of the Chemical Society – Faraday Transactions,* **91** (1995) 2491–2496.
68 T. R. Cundari and E. W. Moody: *Journal of Chemical Information and Computer Sciences,* **37** (1997) 871–875.
69 H. K. D. H. Bhadeshia: *Metal Science* **16** (1982) 159–165.
70 H. S. Rao, J. M. Deshpande and A. Mukherjee: *Science and Engineering of Composite Materials,* **6** (1997) 225–245.
71 E. O. Ezugwu, S. J. Arthur and E. L Hines: *Journal of Materials Processing Technology,* **49** (1995) 225–264.
72 S. Jahanmir: *Machining Science and Technology,* **2** (1998) 137–154.
73 S. E. Martinez, A. E. Smith and B. Bidanda: *Journal of Intelligent Manufacturing,* **5** (1994) 277–286.
74 G. Bonifazi and P. Burrascano: *Advanced Powder Technology,* **5** (1994) 225–239.
75 J. D. Busbee, B. Igelnik, D. Liptak, R. R. Biggers and I. Maartense: *Engineering Applications of Artificial Intelligence,* **11** (1998) 637–647.
76 A. Bensaoula, H. A. Malki and A. M. Kwari: *IEEE Transactions on Semiconductor Manufacturing,* **11** (1998) 421–431.
77. Y. S. Ma, X. Liu, P. F. Gu and J. F. Tang: *Applied Optics,* **35** (1996) 5035–5039.
78. Y. Asada, E. Nakada, S. Matsumoto and H. Uesaka: *Journal of Superconductivity,* **10** (1997) 23–26.
79. M. Q. Feng and F. Y. Bahng: *Journal of Structural Engineering–ASCE,* **125** (1999) 265–271.
80. X. Xu, J. Evans and H. Vanderveldt: *Modelling and Control of Joining Processes,* American Welding Society, Florida, USA, ed. T. Zacharia (1993) 203–214.
81. C. Doyle and G. Fernando: *Smart Materials and Structures,* **7** (1998) 543–549.
82. M. E. Fisher and E. V. Hill: *Materials Evaluation,* **56** (1998) 1395–1401.
83. V. C. Patel, R. W. McClendon and J. W. Goodrum: *Artificial Intelligence Applications,* **10** (1996) 19–28.
84. N. Rai and R. Pitchumani: *Journal of Materials Processing and Manufacturing Science,* **6** (1997) 39–62.
85. S. M. Roberts, J. Kusiak, Y.L. Liu, A. Forcellese and P. J. Withers: *Journal of Materials Processing Technology,* **80–1** (1998) 507–502.
86. W. Hwang, H. C. Park, K. S. Han: *Mechanics of Composite Materials,* **34** (1998) 28–42.
87. S. Cardie and H. K. D. H. Bhadeshia: *Mathematical Modelling of Weld Phenomena 4,* eds H. Cerjak and H. K. D. H. Bhadeshia, The Institute of Materials, London, (1998) 235–255.